CHEMISTRY
A EUROPEAN JOURNAL

DOI: 10.1002/chem.200500552

Oligoethylene Chains Terminated by Ferrocenyl End Groups: Synthesis, Structural Properties, and Two-Dimensional Self-Assembly on Surfaces

Katrin Wedeking,[a] Zhongcheng Mu,[b, c] Gerald Kehr,[a] Jesus Cano Sierra,[a] Christian Mück Lichtenfeld,[a] Stefan Grimme,*[a] Gerhard Erker,*[a] Roland Fröhlich,[a] Lifeng Chi,*[b] Wenchong Wang,[b] Dingyong Zhong,[b] and Harald Fuchs[b]

Abstract: A series of unsaturated long-chain-bridged diferrocenes Fc-$(CH_2)_n$-CH=CH-$(CH_2)_n$-Fc (**4a–e**) was synthesized by means of olefin metathesis. Subsequent catalytic hydrogenation furnished the saturated α,ω-bis-ferrocenyl oligoethylene products Fc-$(CH_2)_m$-Fc (**5**). Members of both series formed highly ordered laminar structures at the highly oriented pyrolytic graphite (HOPG) solid/liquid interface or on the Ag(110) surface, which were characterized by STM. Details of the structural features of these ordered physisorbed surface assemblies of **4** and **5** were analyzed by comparison with DFT calculations on model systems and with the characteristic packing modes of these systems in the crystal.

Keywords: iron · metallocenes · metathesis · scanning tunneling microscopy · self-assembly

Introduction

The defined formation of two-dimensional ordered structures of organic molecules at surfaces is of major current interest in view of the design and development of new functional materials.[1] Chemical pathways to, for example, electronic materials of various kinds will rely on a priori formation of such ordered structures. The organization of purely organic molecules is quite advanced. An often used approach is to attach long saturated hydrocarbon chains to the respective functional organic systems and use their tendency to order through physi/chemisorption at, for example, the liquid/solid interface.[2] Whereas such techniques have successfully been used for the formation of two-dimensionally ordered arrays of organic systems, they have less often addressed metal-containing materials.[3] Such assembly processes might bring metal centers of functional organometallic systems into close proximity in a highly ordered extended periodical structural pattern that could be of interest for future uses in, for example, electronic materials chemistry or surface catalysis. We have begun to investigate possible pathways to such systems and have prepared and characterized physisorbed ordered arrays of oligoethylene-bridged diferrocenes and some closely related substances at the liquid/solid or the solid/gas interface. Some of these first experiments and results are described and discussed here.

Results and Discussion

Synthesis and structural characterization of oligoethylene-linked diferrocenes: Two different synthetic pathways were followed for the preparation of oligoethylene-bridged diferrocenes. The majority of the compounds was obtained by an organometallic olefin metathesis route (see Scheme 1).[4–6] The formation of tetramethylene-bridged diferrocene **5a** may serve as a typical example. Ferrocene was monolithiat-

---

[a] Dipl.-Chem. K. Wedeking, Dr. G. Kehr, Dr. J. Cano Sierra, Dr. C. Mück Lichtenfeld, Prof. Dr. S. Grimme, Prof. Dr. G. Erker, Dr. R. Fröhlich
Organisch-Chemisches Institut der Universität Münster
Corrensstrasse 40, 48149 Münster (Germany)
Fax: (+49) 251-8336503
E-mail: grimmes@uni-muenster.de
erker@uni-muenster.de

[b] Dr. Z. Mu, Prof. Dr. L. Chi, Dr. W. Wang, Dr. D. Zhong, Prof. Dr. H. Fuchs
Physikalisches Institut der Universität Münster
Wilhelm-Klemm-Strasse 10, 48149 Münster (Germany)
Fax: (+49) 251 8333602
E-mail: chi@uni-muenster.de

[c] Dr. Z. Mu
Key Lab for Supramolecular Structure and Materials
College of Chemistry, Jilin University, Changchun 130023 (P. R. China)

Supporting information for this article is available on the WWW under http://www.chemeurj.org/ or from the author.

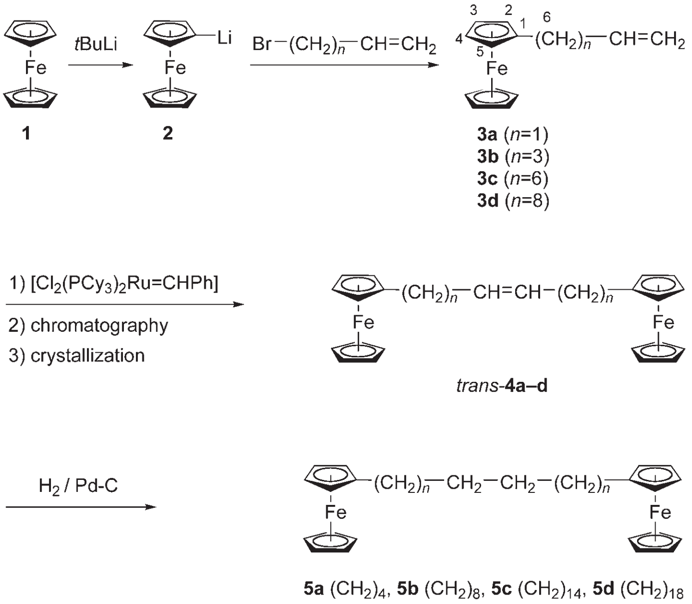

Scheme 1.

ed by treatment with *tert*-butyllithium, as described by Herberhold et al.,[7] and then treated with allyl bromide in THF to yield the allyl ferrocene product **3a**. This was then treated with the [$Cl_2(PCy_3)_2Ru$=CHPh] olefin metathesis catalyst (10 mol%, 5 h at 60 °C in toluene) to give an approximately 3/1 mixture of *trans*-**4a** and *cis*-**4a**. Pure *trans*-1,4-butenediyl-bridged diferrocene **4a** ($FcCH_2CH$=$CHCH_2Fc$) was separated by column chromatography and crystallization and isolated in a yield of about 40%. The corresponding diferrocenes **4b–d** were synthesized analogously. Treatment of lithioferrocene (**2**) with the respective $Br(CH_2)_nCH$=CH_2 reagents (n = 3, 6, 8) gave the corresponding alkenylferrocenes Fc-$(CH_2)_n$-CH=CH_2 (**3b–d**). Subsequent treatment with the [$Cl_2(PCy_3)_2Ru$=CHPh] metathesis catalyst in each case furnished a *trans*/*cis* mixture of coupling products with liberation of ethene. The *trans*-(Fc-$(CH_2)_n$-CH=CH-$(CH_2)_n$-Fc) products *trans*-**4b–d** were again obtained pure after column chromatography and crystallization. They were characterized spectroscopically and by X-ray diffraction (see below). The ^{1}H NMR spectrum of diferrocene product *trans*-**4b** shows a typical appearance. It features the −CH= resonance of the central *trans*-olefin at $\delta = 5.42$ ppm (m, 2H), a ferrocene Cp singlet (10H) at $\delta = 4.01$ ppm, the signals of the C_5H_4 ligand at $\delta = 4.06$ (2,5-H) and 4.03 ppm (3,4-H), and three separate CH_2 multiplets at $\delta = 2.32$ (4H; α-CH_2), 2.03 (4H; γ-CH_2), and 1.57 ppm (4H; β-CH_2).

The central C=C double bond of unsaturated diferrocenes **4a–d** was selectively hydrogenated (H_2, Pd/C in THF at ambient temperature) to give high yields (mostly >90%) of saturated diferrocenes of the composition Fc-$(CH_2)_m$-Fc (**5a–d** with $m = 4$, 8, 14, and 18, respectively). The typical ^{13}C NMR spectrum of compound **5b** features a Cp resonance at $\delta = 68.8$ ppm, three signals of the monosubstituted cyclopentadienide moiety at $\delta = 89.6$ (C1), 68.4 (C2, C5), and 67.5 ppm (C3, C4), and four separate $^{13}CH_2$ NMR signals of the four symmetry-equivalent pairs of methylene groups of the bridging −$(CH_2)_8$− chain ($\delta = 31.7$, 30.01, 29.97, 29.93 ppm).

The diferrocene with the longest unsaturated bridging chain, Fc-$(CH_2)_{10}$-CH=CH-$(CH_2)_{10}$-Fc (**4e**), was prepared differently. In this case olefin metathesis was carried out prior to attachment of the long bridging chain to the ferrocene nucleus. The starting material 1-bromo-11-dodecene (**6**)[8] underwent olefin metathesis (1 mol% [$Cl_2(PCy_3)_2Ru$=CHPh] in toluene at room temperature) to yield a 3:1 mixture of *trans*- and *cis*-1,22-dibromo-11-docosene (**7**). Pure *trans*-**7** was obtained by crystallization from heptane. It was treated with about three molar equivalents of ferrocenyllithium (**2**) to give *trans*-Fc-$(CH_2)_{10}$-CH=CH-$(CH_2)_{10}$-Fc (**4e**) in about 40% yield after chromatography (see Scheme 2).

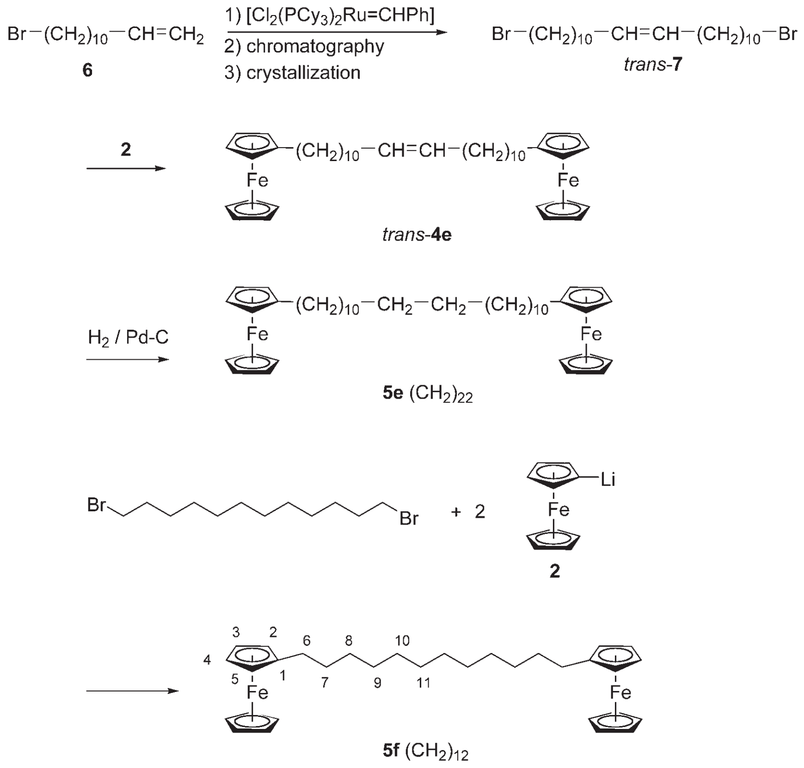

Scheme 2.

Catalytic hydrogenation of **4e** (H_2, Pd/C, THF) furnished the saturated derivative Fc-$(CH_2)_{22}$-Fc (**5e**) in 94% yield. One additional saturated oligoethylene-bridged diferrocene was prepared in a similar way, namely, Fc-$(CH_2)_{12}$-Fc (**5f**). In this case lithioferrocene (**2**) was treated with 1,12-dibromododecane. From the reaction mixture the product Fc-$(CH_2)_{12}$-Fc (**5f**) was isolated after chromatography and crystallization (27% yield; see Scheme 2).

The unsaturated *trans*-alkenediyl-bridged diferrocenes **4a–e** were characterized by X-ray crystal structure analyses. Figure 1 shows the molecular structures of these compounds

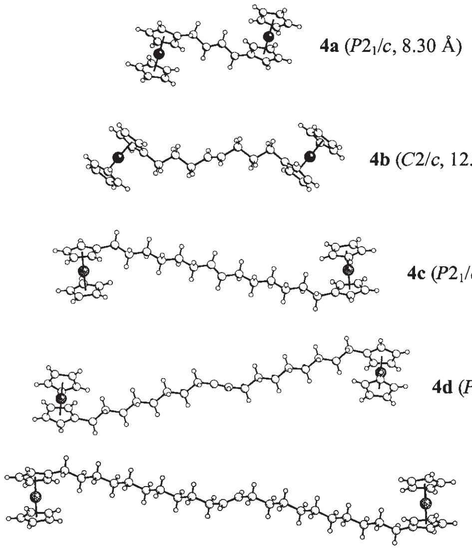

Figure 1. Comparison of the molecular structures of the *trans*-Fc-$(CH_2)_n$-CH=CH-$(CH_2)_n$-Fc compounds **4a–e** in the crystal (with space group and intramolecular $Cp_{(centroid)}\cdots Cp_{(centroid)}$ distances between the C_5H_4 groups).

in the solid state. All the connecting hydrocarbon chains are in their maximally extended conformations with antiperiplanar orientations of all saturated $C(sp^3)$–$C(sp^3)$ linkages. In all compounds the ferrocenyl units at the termini of the connecting hydrocarbon chain are oriented parallel to each other with their $Cp_{(centroid)}$-Fe-$Cp_{(centroid)}$ vectors close to perpendicular to the connecting hydrocarbon chain. In the observed orientation in the crystal packing of each of these molecules the -$(CH_2)_n$-CH=CH-$(CH_2)_n$- chain connects an "upper" Cp ring of one ferrocene unit with a "lower" cyclopentadienide in this orientation with a parallel intramolecular arrangement of the $Cp_{(centroid)}$-Fe-$Cp_{(centroid)}$ vectors (see Figure 1).

The saturated oligoethylene-bridged diferrocenes **5a–e** were also characterized by X-ray diffraction (Figure 2). They behave structurally as if a respective section were cut from a polyethylene chain and its ends "stoppered" by the organometallic ferrocenyl end groups. In all compounds the -$(CH_2)_m$- chains are in maximal extension (all-antiperiplanar alkane conformations). The projections depicted in Figure 2 show that the $Cp_{(centroid)}$-Fe-$Cp_{(centroid)}$ vectors of **5a** (C_4-bridged), **5c** (C_{14}), **5d** (C_{18}), and **5e** (C_{22}) are intramolecularly arranged parallel to each other, and again "upper" Cp rings on one end are connected to "lower" Cp rings at the other end of the chain in this extended orientation. Only the conformational orientation of Fc-$(CH_2)_8$-Fc (**5b**) is different. Here the $Cp_{(centroid)}$-Fe-$Cp_{(centroid)}$ vectors are in an almost perpendicular relative orientation (see Figure 2). This probably means that both the parallel and the perpendicular orientations are energetically not much separated. This will be of importance for the interpretation of the surface assembly of these systems (see below).

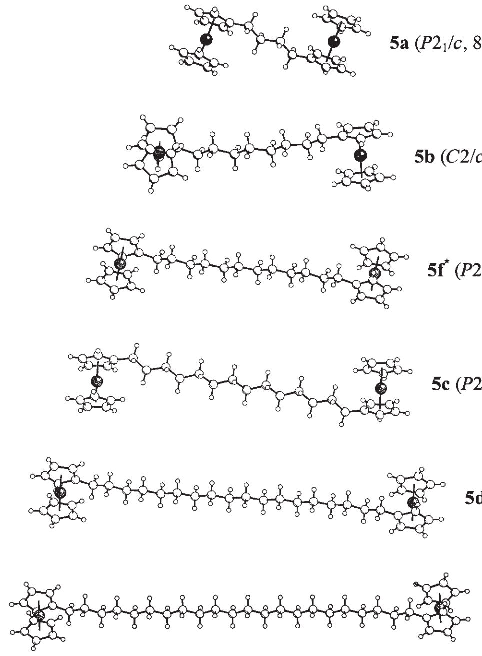

Figure 2. Comparison of the molecular structures of the Fc-$(CH_2)_m$-Fc compounds **5a–f** in the crystal (with space group and intramolecular $Cp_{(centroid)}\cdots Cp_{(centroid)}$ distances between the C_5H_4 groups). Compound **5f** was measured at room temperature; at −75 °C a first-order phase transition resulted in decomposition of the crystal.

The crystal packing of all these compounds shows characteristic parallel arrangements of the long oligoethylene chains. This is illustrated by views of the packing pattern of Fc-$(CH_2)_{18}$-Fc (**5d**) from two different directions (Figures 3 and 4; see also Supporting Information). A skew projection onto the *ac* plane shows parallel arrangements of the -$(CH_2)_{18}$- chains (C–C 7.59 Å). The ferrocenyl units are all oriented with their $Cp_{(centroid)}$-Fe-$Cp_{(centroid)}$ vectors perpendicular to the mean -$(CH_2)_{18}$- vectors (see Figure 3). The Fe···Fe separations between parallel Fc-$(CH_2)_{18}$-Fc chains are 7.59 Å. The ferrocenyl units of the pairs of the resulting Fc-$(CH_2)_{18}$-Fc ribbons are close together with calculated Fe···Fe distances of 5.85 Å (see Figure 3).

Figure 4 shows a different view of the packing with a relative arrangement of different next neighbors in the unit cell. In this arrangement the -$(CH_2)_{18}$- chains are rather close together (closest C···C distance between two chains: 4.14 Å, longest C···C distance between two chains: 4.81 Å). The ferrocenyl units within the ribbons exhibit an alternating ste-

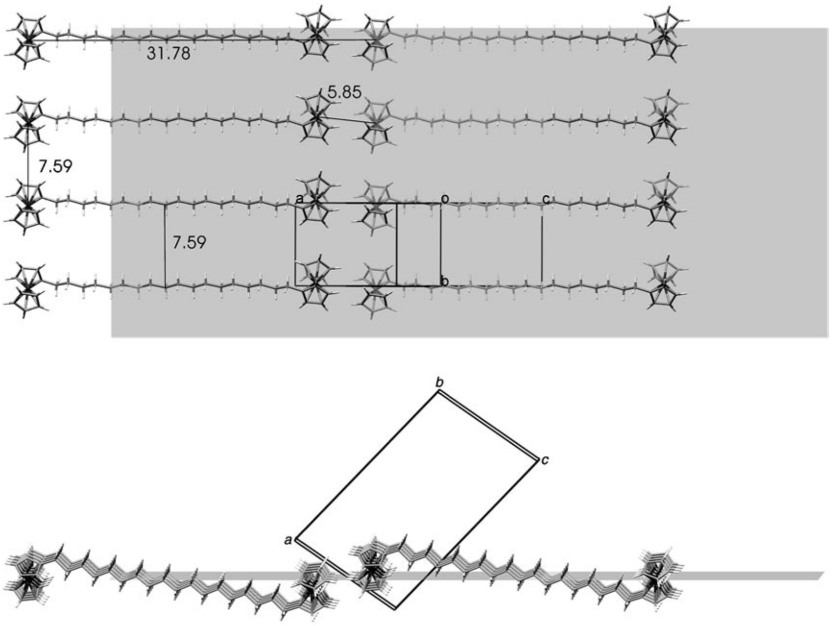

Figure 3. Crystal packing arrangement of the individual Fc-$(CH_2)_{18}$-Fc chains of **5d** (views onto the plane parallel to the *b* axis from two angles are depicted).

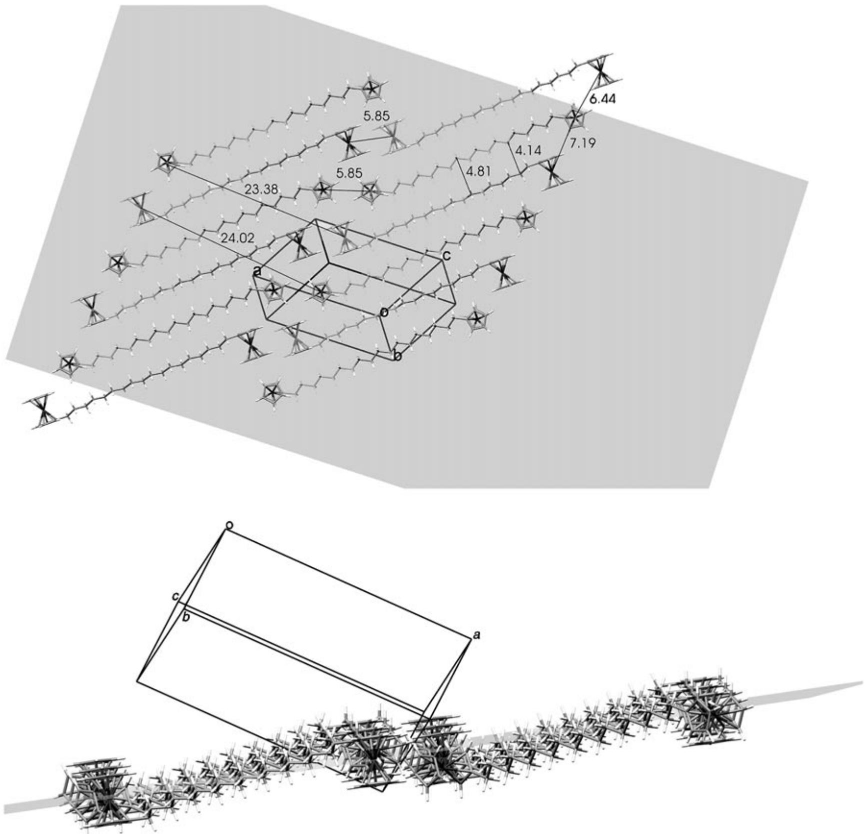

Figure 4. Two projections of the intermolecular arrangement of the nearest-neighbor molecules of Fc-$(CH_2)_{18}$-Fc compound **5d** in the crystal.

reochemical orientation with their $Cp_{(centroid)}$-Fe-$Cp_{(centroid)}$ vectors close to normal to each other and intraribbon Fe···Fe separations of 7.19 und 6.44 Å. The ferrocenes between adjacent ribbons are arranged parallel and feature a Fe···Fe distance of 5.85 Å. The oriented -$(CH_2)_{18}$- chains form an angle of about 50° with the hypothetical vector along which the ferrocenyl units are aligned (see Figure 4).

Surface assembly of the bridged diferrocenes: Our STM experiments were carried out with the diferrocenes linked with sufficiently long hydrocarbon chains. We first investigated their assembly at the solid/liquid interface using highly oriented pyrolytic graphite (HOPG). Saturated solutions of **4** or **5** were added to the surface of freshly conditioned HOPG, and the resulting ordered Fc-R-Fc monolayers investigated by STM.

The long bridging hydrocarbon chain is essential to observe ordered physisorption of the Fc-R-Fc compounds **4** and **5** at the HOPG/phenyloctane solid/liquid interphase. With the shorter chains, for example, **5a** (Fc-$(CH_2)_4$-Fc) and **5b** (Fc-$(CH_2)_8$-Fc) we did not observed an ordered STM image under our experimental conditions. Also for the unsaturated system **4c** (*trans*-Fc-$(CH_2)_6$-CH=CH-$(CH_2)_6$-Fc), no stable STM image on the HOPG surface was obtained. However, the saturated compounds **5f**, **5c**, and **5d** (Fc-$(CH_2)_m$-Fc, with $m = 12$, 14, and 18) gave highly ordered physisorbed monolayers on HOPG, as observed by STM.

Figure 5 depicts an STM image of a **5c** (Fc-$(CH_2)_{14}$-Fc) monolayer on HOPG. The laminar structure of the adsorbed molecular monolayer is clearly visible. The periodicity of the laminar pattern is about 2.2 nm, which matches well with the molecular dimensions of the individual molecules of **5c** (the $Cp_{(centroid)}\cdots Cp_{(centroid)}$ distance in the extended conformation of **5c** found in the crystal is 21.3 Å, see above). The rows of bright spots in the image

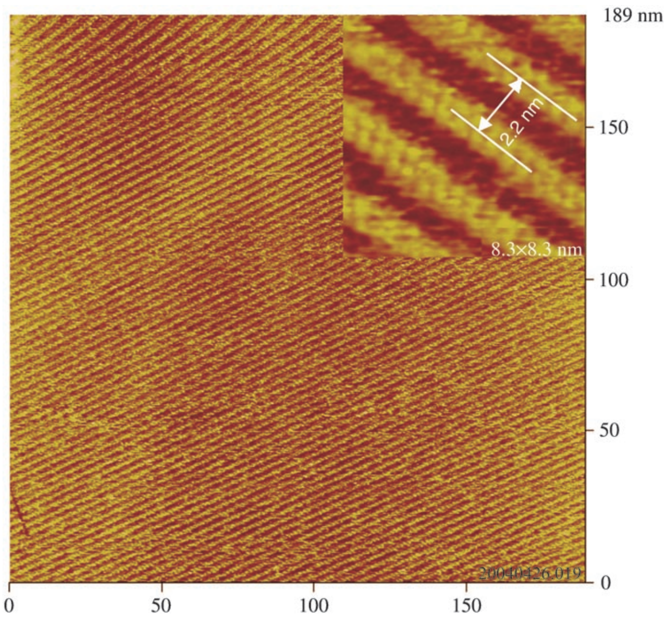

Figure 5. STM image of **5c** (Fc-(CH$_2$)$_{14}$-Fc) on HOPG.

may represent places where the ferrocenyl head groups of **5c** are located in this pattern. Thus, the overall appearance of the pattern of the Fc-(CH$_2$)$_{14}$-Fc (**5c**) molecules physisorbed on the HOPG surface seems to be similar to their general arrangement in the crystal: It appears that double rows of ferrocenyl head groups are assembled close to each other.

The pattern of physisorbed Fc-(CH$_2$)$_{18}$-Fc (**5d**) on HOPG is similar (Figure 6). The bright features in the close-up image may again originate from the ferrocenyl double rows. The lateral separation between the individual chains is about 6 Å. In this case the direction of the -(CH$_2$)$_{18}$- chains seems to form an angle of ca. 60° with the vector of alignment of the ferrocenyl groups. The rows of bright ferrocenyl features in this case are about 2.7 nm apart. Again, the image of the laminar pattern of the physisorbed Fc-(CH$_2$)$_{18}$-Fc molecules bears some resemblance to the general packing pattern observed for **5d** in the crystal (see above).

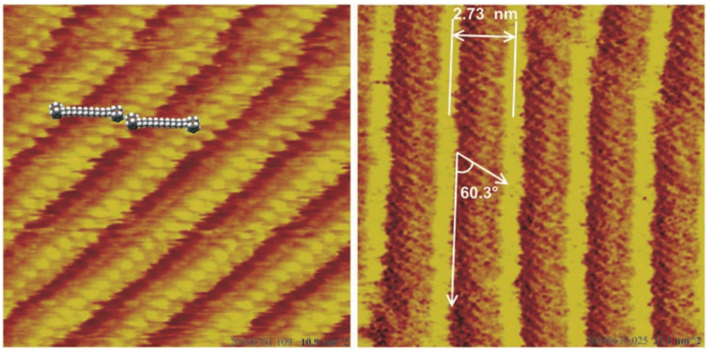

Figure 6. STM images of Fc-(CH$_2$)$_{18}$-Fc (**5d**) on HOPG with a projection of a pair of molecular models (left).

The unsaturated *trans*-Fc-(CH$_2$)$_n$-CH=CH-(CH$_2$)$_n$-Fc compounds form physisorbed ordered monolayers of a similar appearance when the connecting chains are of sufficient length, but they are in general more difficult to image by STM. We have observed STM images of the laminar surface structures of *trans*-**4d** and *trans*-**4e**. Figure 7 provides two views of the pattern obtained from *trans*-Fc-(CH$_2$)$_8$-CH=CH-(CH$_2$)$_8$-Fc (**4d**). In the close-up view the typical pattern of the double rows of ferrocenyl end groups again shows up as poorly resolved rows of bright spots.

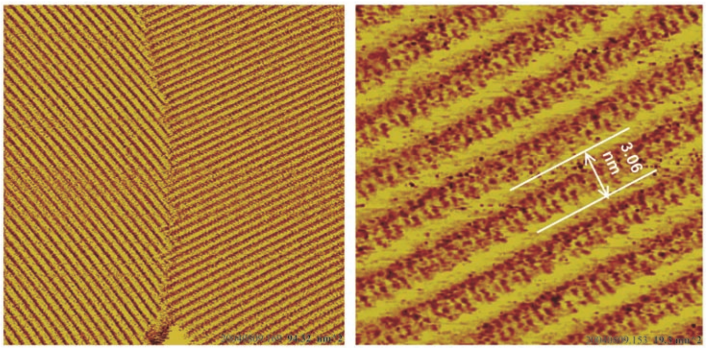

Figure 7. Overview (left) and close-up (right) STM images of the surface pattern of *trans*-Fc-(CH$_2$)$_8$-CH=CH-(CH$_2$)$_8$-Fc (**4d**) at the HOPG/phenyloctane interface.

Analogous ordered laminar structures could be obtained by depositing *trans*-Fc-(CH$_2$)$_6$-CH=CH-(CH$_2$)$_6$-Fc (**4c**) on an Ag(110) surface by molecular beam expitaxy under ultrahigh vacuum (UHV). The bright spots in the UHV STM image of *trans*-**4c** on Ag(110) again may represent the double rows of ferrocenyl end groups (Figure 8). In the surface structure of unsaturated *trans*-Fc-(CH$_2$)$_6$-CH=CH-(CH$_2$)$_6$-Fc, additional prominent features appear periodically in the center of the dark intermediate areas between the bright rows of ferrocenyl features.

The STM experiments revealed that the hydrocarbon-bridged diferrocenes *trans*-**4** and **5** form ordered laminar structures at the HOPG surface if the connecting chains are of sufficient length that feature overall structural arrangements similar to those observed for such compounds in the crystal, with the long hydrocarbon chains arranged parallel to each other and the ferrocenyl head groups oriented closely together. From the analysis of the crystal packing (see above) it could, however, not be decided whether a structure in which the ferrocene subunits are oriented with their major Cp$_{\text{(centroid)}}$-Fe-Cp$_{\text{(centroid)}}$ vectors parallel or orthogonal would be favored at the surface. Since the resolution of the STM images was insufficient to distinguish between these structural alternatives, we used a quantum chemical approach to possibly solve this interesting problem.

The self-assembly of the diferrocene derivatives on a planar graphite surface was approached by model DFT calculations.[9] Since most functionals fail in the description of

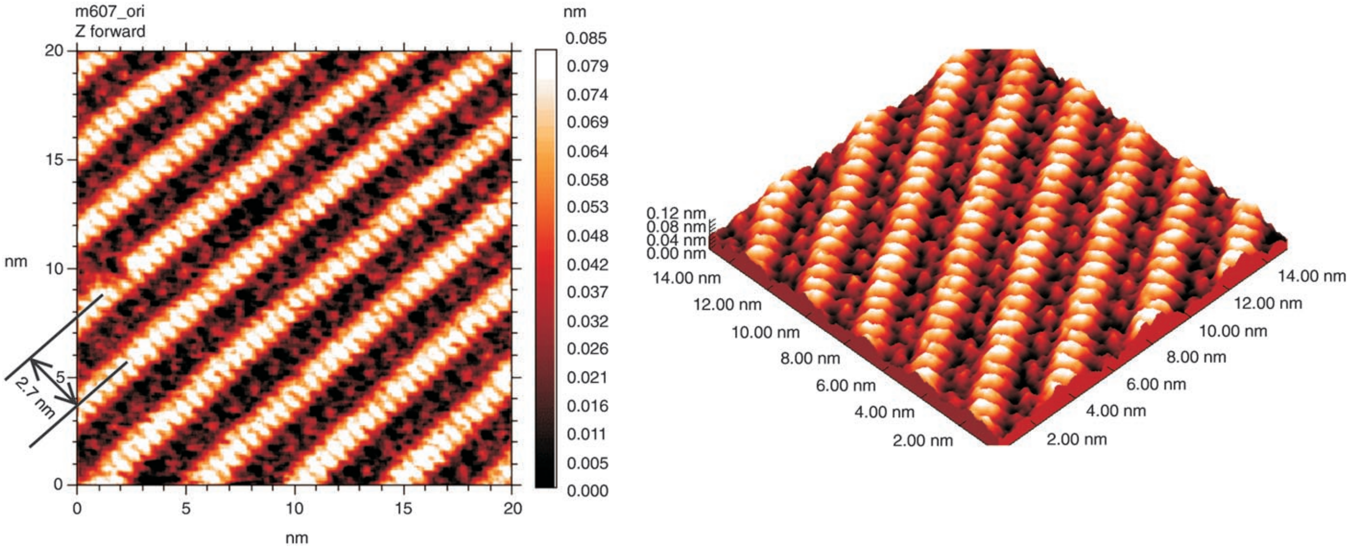

Figure 8. UHV-STM images of the pattern of *trans*-Fc-$(CH_2)_6$-CH=CH-$(CH_2)_6$-Fc (**4c**) molecules deposited on an Ag(110) surface.

attractive dispersion (van der Waals) forces, we used a recently proposed empirical approach (DFT-D)[10] that corrects this behavior. All complexes shown are only stable due to the dispersion correction and have positive DFT binding energies.

We first determined the dimerization energy of a pair of ferrocene molecules in the gas phase[11] (Figure 9a) in two alternative orientations. These correspond grossly to the possible arrangements of the ferrocene units in crystals of the oligoethylene-linked diferrocenes (see above). In the gas phase the ferrocene dimer favors the orthogonal orientation ($\mathbf{1}_2^{\text{par}}$), which allows for a shorter metal–metal distance (5.045 Å) than its parallel isomer $\mathbf{1}_2^{\text{par}}$ (5.520 Å). In the $\mathbf{1}_2^{\text{ort}}$ dimer, one Cp ring fills a gap near the metal atom of the second monomer, and thus a calculated angle of 72° results between the Fe–Fe and $\text{Cp}_{\text{(centroid)}}$-Fe-$\text{Cp}_{\text{(centroid)}}$ vectors. The parallel orientation $\mathbf{1}_2^{\text{par}}$ is only 1.2 kcal mol^{-1} less stable. The gas-phase dimerization energies of **1** are comparable with that of naphthalene (5.3 kcal mol^{-1} with DFT-D-BYLP).[10] Closer inspection (energy decomposition) of the interactions reveals that dispersion, electrostatic, and orbital interactions stabilize $\mathbf{1}_2^{\text{ort}}$ more than $\mathbf{1}_2^{\text{par}}$, which has lower Pauli repulsion, probably due to the greater distance between the monomers (for further details see the Supporting Information).

The physisorption of ferrocene on graphite was modeled by DFT with coronene ($C_{24}H_{12}$) as substrate for ferrocene and a larger polycyclic compound ($C_{40}H_{16}$) for the ferrocene dimer. The ferrocene molecule has a relatively large binding energy (-9.5 kcal mol^{-1}) to coronene and prefers C–H···π interactions[11] ("T-shaped") with the aromatic system (Figure 9b). Compared to the binding energy of the T-shaped benzene dimer (-2.1 kcal mol^{-1} with DFT-D-BLYP),[10] more C–H···π interactions and larger dispersion contributions stabilize $(\mathbf{1}{\cdot}C_{24}H_{12})^{\text{T}}$. The stacked complex $(\mathbf{1}{\cdot}C_{24}H_{12})^{\text{S}}$ is less favored by 1.1 kcal mol^{-1} in the DFT-D calculation. Its dispersion, electrostatic, and orbital interactions are smaller than those of $(\mathbf{1}{\cdot}C_{24}H_{12})^{\text{T}}$.

To analyze how a pair of adjacent ferrocene molecules might interact in a nonbonding situation on graphite, we reoptimized the ferrocene dimers on a larger graphite model ($C_{40}H_{16}$, Figure 9c). Similar to the gas phase, the orthogonal orientation of the $\text{Cp}_{\text{(centroid)}}$-Fe-$\text{Cp}_{\text{(centroid)}}$ vectors was found to be more favorable, now by 3.1 kcal mol^{-1}. Binding of the orthogonal dimer $\mathbf{1}_2^{\text{ort}}$ on this substrate is 1.9 kcal mol^{-1} more favorable than of the parallel dimer $\mathbf{1}_2^{\text{par}}$, which is preferentially bound by C–H···π interactions to the substrate. These results show that the interaction with the aromatic system adds additional relative stabilization to the orthogonal dimer. We would therefore expect neighboring ferrocenes on a HOPG surface to prefer a similar orientation with the $\text{Cp}_{\text{(centroid)}}$-Fe-$\text{Cp}_{\text{(centroid)}}$ vectors arranged preferentially normal to each other, although other relative arrangements seem possible in view of the small energy differences involved.

Conclusion

We have shown that unsaturated *trans*-Fc-$(CH_2)_n$-CH=CH-$(CH_2)_n$-Fc compounds **4** are readily available, for example, by olefin metathesis routes from the respective alkenylferrocene precursors. The catalytic hydrogenation of **4** furnished a series of oligoethylene-bridged diferrocenes **5**. Both these series of molecules form highly ordered physisorbed structures at the solid/liquid or solid/gas interface. These have a laminarlike appearance. It seems that the ferrocenyl end groups in these ordered structures are oriented along a vector in a defined angle to the direction of the bridging hydrocarbon chains. We thus were able to orient metal-containing chemical building blocks at a surface in well-defined patterns. It is even possible to introduce functional groups

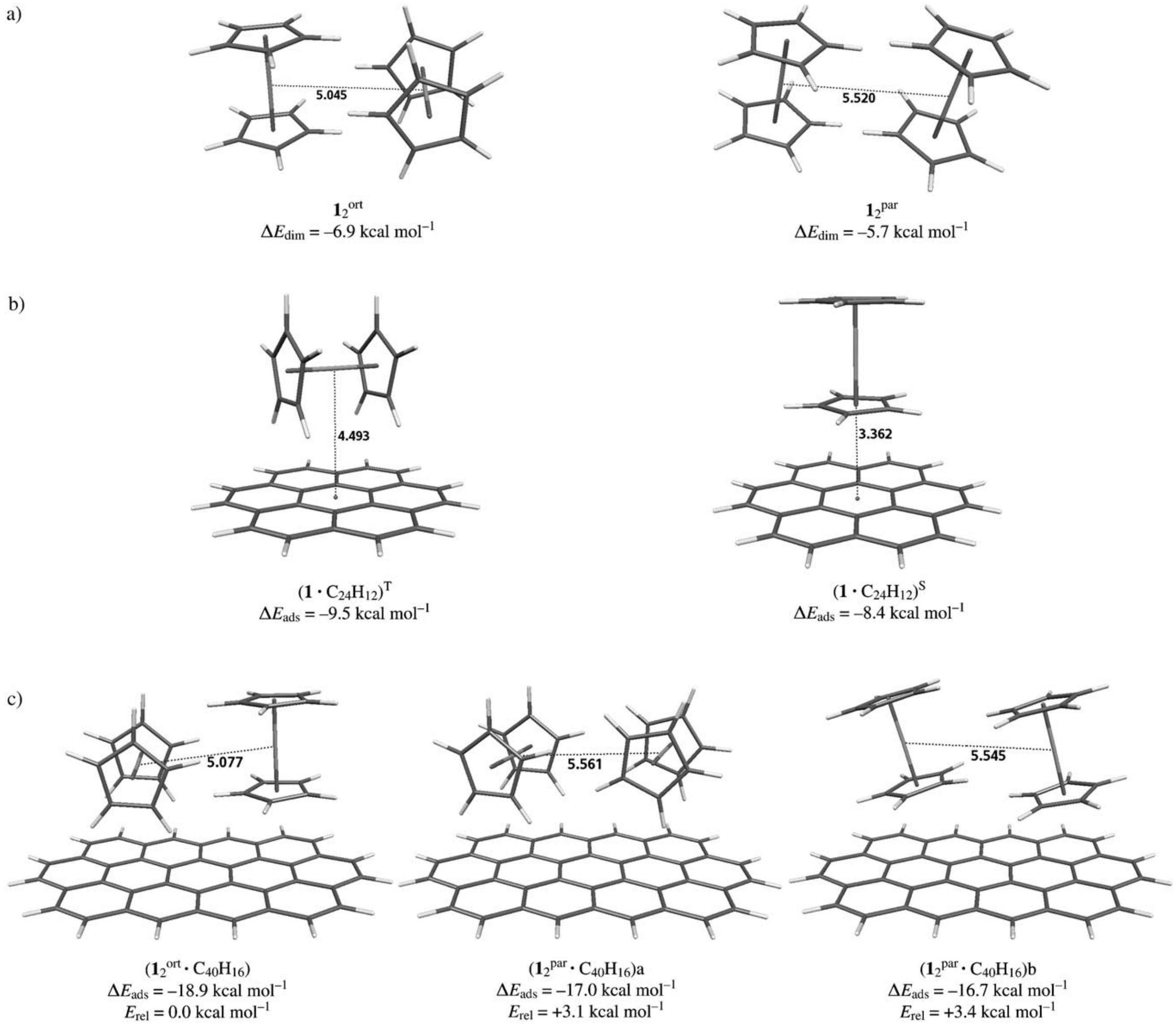

$\mathbf{1}_2^{\text{ort}}$
$\Delta E_{\text{dim}} = -6.9$ kcal mol^{-1}

$\mathbf{1}_2^{\text{par}}$
$\Delta E_{\text{dim}} = -5.7$ kcal mol^{-1}

$(\mathbf{1}\cdot C_{24}H_{12})^{T}$
$\Delta E_{\text{ads}} = -9.5$ kcal mol^{-1}

$(\mathbf{1}\cdot C_{24}H_{12})^{S}$
$\Delta E_{\text{ads}} = -8.4$ kcal mol^{-1}

$(\mathbf{1}_2^{\text{ort}}\cdot C_{40}H_{16})$
$\Delta E_{\text{ads}} = -18.9$ kcal mol^{-1}
$E_{\text{rel}} = 0.0$ kcal mol^{-1}

$(\mathbf{1}_2^{\text{par}}\cdot C_{40}H_{16})$a
$\Delta E_{\text{ads}} = -17.0$ kcal mol^{-1}
$E_{\text{rel}} = +3.1$ kcal mol^{-1}

$(\mathbf{1}_2^{\text{par}}\cdot C_{40}H_{16})$b
$\Delta E_{\text{ads}} = -16.7$ kcal mol^{-1}
$E_{\text{rel}} = +3.4$ kcal mol^{-1}

Figure 9. DFT-D (BLYP/TZVP) calculated structures of ferrocene dimer and physisorption on graphite model compounds. a) Ferrocene dimer with orthogonal and parallel orientation of the Fe(Cp)$_2$ units. b) Ferrocene monomer on coronene ($C_{24}H_{12}$): T-shaped (T) and stacked (S) conformers. c) Ferrocene dimers on $C_{40}H_{16}$: orthogonal and two isomers of adsorbed parallel dimer. Adsorption energies are given for the respective dimers. Relative energies are given for the three structural isomers shown.

within the connecting chains, which may eventually allow these structures to be fixed, for example, by chemical cross-linking.[12] This may open pathways to generate functionalized surfaces from readily available suitable organometallic precursors.

Experimental Section

General: All reactions with air- and moisture-sensitive compounds were carried out under dry argon in Schlenk-type glassware or in a glove box. Solvents were dried and distilled prior to use. Commercially available reagents were used as received (Fluka: allyl bromide, $[Cl_2(PCy_3)_2Ru{=}CHPh]$; Aldrich: 5-bromo-1-pentene, 8-bromo-1-octene, 10-bromo-1-decene). 1-Bromo-11-dodecene (**6**) was prepared according to a literature procedure.[8] For additional general conditions, including a list of instruments used for physical characterization of the compounds, see ref. [6]. Most NMR assignments were secured by a variety of 2D NMR experiments.[13]

Data sets were collected with a Nonius KappaCCD diffractometer, equipped with a rotating-anode generator. Programs used: data collection COLLECT (Nonius B.V., 1998), data reduction Denzo-SMN (Z. Otwinowski, W. Minor, *Methods Enzymol*. **1997**, *276*, 307–326), absorption correction SORTAV (R. H. Blessing, *Acta Crystallogr. Sect. A* **1995**, *51*, 33–37; R. H. Blessing, *J. Appl. Crystallogr*. **1997**, *30*, 421–426) and Denzo (Z. Otwinowski, D. Borek, W. Majewski, W. Minor, *Acta Cryst. Sect. A* **2003**, *59*, 228–234), structure solution SHELXS-97 (G. M. Sheldrick, *Acta Crystallogr. Sect. A* **1990**, *46*, 467–473), structure refinement SHELXL-97 (G. M. Sheldrick, Universität Göttingen, **1997**), graphics SCHAKAL (E. Keller, Universität Freiburg, **1997**) and CCDC-MERCURY V1.3.[14]

CCDC-268624 (**4a**), CCDC-268625 (**4b**), CCDC-268626 (**4c**), CCDC-268627 (**4d**), CCDC-268628 (**4e**), CCDC-268629 (**5a**), CCDC-268630 (**5b**), CCDC-268631 (**5c**), CCDC-268632 (**5d**), CCDC-268633 (**5e**), and CCDC-270036 (**5f**) contain the supplementary crystallographic data for this paper. These data can be obtained free of charge from the Cambridge Crystallographic Data Centre via www.ccdc.cam.ac.uk/data_request/cif.

DFT calculations: The calculations were performed with the TURBOMOLE 5.6 suite of programs (Universität Karlsruhe, **2003**). The structures were fully optimized at the DFT level employing the B-LYP functional (A. D. Becke, *Phys. Rev. A*. **1988**, *38*, 3098–3100, C. Lee, W. Yang, R. G. Parr, *Phys. Rev. B*, **1988**, *37*, 785–789). A Gaussian AO basis of valence-triple-zeta quality including polarization functions (TZVP) (A. Schäfer, C. Huber, R. Ahlrichs, *J. Chem. Phys.* **1994**, *100*, 5829–5835) was used for all atoms. The RI approximation was used for the two-electron integrals (K. Eichkorn, O. Treutler, H. Öhm, M. Häser, R. Ahlrichs, *Chem. Phys. Lett.* **1995**, *240*, 283–290.)

STM analysis: The STM used in the experiment at the liquid/solid interface was a commercial instrument (Digital Instruments, NanoScope III). HOPG (Grade ZYB, mosaicity 0.8±0.2 deg) and STM tip (Pt/Ir 90/10 wire) were bought from Material-Technologie & Kristalle (MaTeck) GmbH, Jülich, Germany.

Phenyloctane was selected as solvent because of its low vapor pressure and nonpolarity. A drop of a saturated solution of the material was applied to a slab of freshly cleaved HOPG with a Pasteur pipette. The drop slipped off of the substrate leaving an liquid film on the surface into which the STM tip was immersed. The physisorbed 2D crystal structure was investigated at the solid/liquid interface using STM.

The monolayer films on Ag(110) were prepared by using organic molecular beam deposition (OMBD) under ultrahigh vacuum (UHV) with a base vacuum of about 10^{-9} Torr. The substrates were cleaned by Ar^+ sputtering (500 eV, 15 min) and then annealed to 800 K. Before deposition, the organic materials were degassed and purified in OMBD crucibles under UHV by heating to their sublimation temperatures (120 °C for $Fc(CH_2)_6CH{=}CH(CH_2)_6Fc$ (**4c**)) and maintaining this temperature for more than 3 h. The purified material was then sublimed onto the cleaned metallic substrate at room temperature with a deposition rate of about 0.2 mL min^{-1}. The as-prepared monolayer films were then investigated by scanning tunneling microscopy (Omicron) under UHV at room temperature. Tungsten tips obtained by electrochemical etching were used for the STM experiments.

$Fc\text{-}CH_2CH{=}CH_2$ (3a): The monolithiation of ferrocene (**1**) was carried out under the conditions described by Herberhold et al.,[7] using ferrocene (11.2 g, 60 mmol) and *tert*-butyllithium (1.5 M in pentane, 40 mL, 60 mmol) in tetrahydrofuran (80 mL) under argon. The generated lithioferrocene (**2**) was used in situ. Tetrahydrofuran (100 mL) was added, and the solution cooled to −78 °C. Allyl bromide (4.80 g, 40 mmol) was added slowly via syringe, and the reaction mixture stirred for 16 h, while slowly warming to room temperature. The solvent was removed under reduced pressure. The residue was dissolved in pentane, the solvent volume reduced, and the remaining ferrocene (**1**) was allowed to crystallize out of the mixture. Compound **3a** remained in solution. Afterwards the crude product was purified by column chromatography on silica gel. (pentane). The second fraction was collected. (R_f (**1**)=0.34; R_f (**3a**)=0.30) After evaporation of the solvent compound **3a** was obtained as a red liquid (1.80 g, 20 %) that contained ca. 15 % of ferrocene (removed after the subsequent metathesis coupling step, see below). ^{1}H NMR (599.8 MHz, 298 K, C_6D_6): δ=5.94 (ddt, $^3J_{H,H}$=17.0 Hz, $^3J_{H,H}$=10.3 Hz, $^3J_{H,H}$=6.7 Hz, 1 H; 7-H), 5.01 (dm, $^3J_{H,H}$=17.0 Hz, 1 H; 8-H$_Z$), 4.98 (dm, $^3J_{H,H}$=10.2 Hz, 1 H; 8-H$_E$), 3.99 (s, 5 H; Cp-H), 3.94 (s, 4 H; 2,3,4,5-H), 2.93 ppm (dt, $^3J_{H,H}$=6.7 Hz, $^4J_{H,H}$=1.5 Hz, 2 H; 6-H); ^{13}C NMR (150.8 MHz, 298 K, C_6D_6): δ=137.9 (C7), 115.1 (C8), 87.1 (C1), 68.8 (Cp), 68.3 (C2, C5), 67.7 (C3, C4), 34.0 ppm (C6); MS (MALDI-TOF (DCTB)): *m/z* (%): 226.0 (100) [M^+].

$Fc\text{-}(CH_2)_3\text{-}CH{=}CH_2$ (3b): Compound **3b** was prepared analogously to the procedure described for **3a** using 5-bromo-1-pentene (5.00 g, 33.6 mmol), ferrocene (**1**, 9.35 g, 50 mmol), and *tert*-butyllithium (1.5 M in pentane, 34 mL, 50 mmol). After column chromatography on silica gel (pentane), compound **3b** was obtained as a red liquid (R_f (**1**)=0.34; R_f (**3b**)=0.28) (1.43 g, 28 %) that contained ca. 15 % of ferrocene (removed after the subsequent metathesis coupling step, see below). ^{1}H NMR (400 MHz, 300 K, C_6D_6): δ=5.76 (ddt, $^3J_{H,H}$=17.2 Hz, $^3J_{H,H}$=10.2 Hz, $^3J_{H,H}$=6.7 Hz, 1 H; 9 H), 5.03 (dm, $^3J_{H,H}$=17.2 Hz, 1 H; 10-H$_Z$), 4.99 (dm, $^3J_{H,H}$=10.2 Hz, 1 H; 10-H$_E$), 3.99 (s, 5 H; Cp-H), 3.94 (s, 4 H; 2,3,4,5-H), 2.21 (m, 2 H; 6-H), 2.00 (m, 2 H; 8-H), 1.54 ppm (m, 2 H; 7-H); ^{13}C NMR (101 MHz, 300 K, C_6D_6): δ=139.3 (C9), 115.3 (C10), 89.5 (C1), 69.2 (Cp), 68.8 (C2, C5), 67.9 (C3, C4), 34.3 (C8), 31.2 (C7), 29.7 ppm (C6).

$Fc\text{-}(CH_2)_6\text{-}CH{=}CH_2$ (3c): Compound **3c** was prepared analogously to the procedure described for **3a** using 8-bromo-1-octene (3.24 g, 17 mmol), ferrocene (**1**, 3.5 g, 18.8 mmol), and *tert*-butyllithium (1.5 M in pentane, 12.5 mL, 18.8 mmol) After column chromatography on silica gel (pentane), compound **3c** was obtained as a red liquid (R_f (**1**)=0.35; R_f (**3c**)=0.30) (1.43 g, 28 %) that contained ca. 15 % of ferrocene (removed after the subsequent metathesis coupling step, see below). ^{1}H NMR (599.8 MHz, 298 K, C_6D_6): δ=5.78 (ddt, $^3J_{H,H}$=17.0 Hz, $^3J_{H,H}$=10.3 Hz, $^3J_{H,H}$=6.6 Hz, 1 H; 12-H), 5.04 (dm, $^3J_{H,H}$=17.0 Hz, 1 H; 13-H$_Z$), 4.99 (dm, $^3J_{H,H}$=10.1 Hz, 1 H; 13-H$_E$), 4.02 (s, 5 H; Cp-H), 3.98 (pt, 2 H; 2,5-H), 3.96 (pt, 2 H; 3,4-H), 2.25 (m, 2 H; 6-H), 1.98 (m, 2 H; 11-H), 1.47 (m, 2 H; 7-H), 1.31 (m, 2 H; 10-H), 1.25 ppm (m, 4 H; 8,9-H); ^{13}C NMR (150.8 MHz, 298 K, C_6D_6): δ=139.2 (C12), 114.5 (C13), 89.5 (C1), 68.8 (Cp), 68.4 (C2, C5), 67.5 (C3, C4), 34.2 (C11), 31.6 (C7), 30.0 (C6), 29.8 (C8), 29.4 (C9), 29.2 ppm (C10); MS (MALDI-TOF (DCTB)): *m/z* (%): 296.0 (100) [M^+].

$Fc\text{-}(CH_2)_8\text{-}CH{=}CH_2$ (3d): Compound **3d** was prepared analogously to the procedure described for **3a** using 10-bromo-1-decene (5 g, 22.9 mmol), ferrocene (**1**, 8.6 g, 45 mmol), and *tert*-butyllithium (1.5 M in pentane, 30 mL, 45 mmol). After column chromatography on silica gel (pentane), compound **3d** was obtained as a red liquid (R_f (**1**)=0.35; R_f (**3d**)=0.30) (3.66 g, 49 %) that contained about 15 % of ferrocene (removed after the subsequent metathesis coupling step, see below). ^{1}H NMR (599.8 MHz, 298 K, C_6D_6): δ=5.79 (ddt, $^3J_{H,H}$=17.1 Hz, $^3J_{H,H}$=10.4 Hz, $^3J_{H,H}$=6.6 Hz, 1 H; 14-H), 5.04 (dm, $^3J_{H,H}$=17.1 Hz, 1 H; 15-H$_Z$), 4.99 (dm, $^3J_{H,H}$=10.4 Hz, 1 H; 15-H$_E$), 4.02 (s, 5 H; Cp-H), 3.99 (pt, 2 H; 2,5-H), 3.96 (pt, 2 H; 3,4-H), 2.26 (m, 2 H; 6-H), 1.99 (m, 2 H; 13-H), 1.49 (m, 2 H; 7-H), 1.32 (m, 2 H; 12-H), 1.24 ppm (m, 8 H; 8,9,10,11-H); ^{13}C NMR (150.8 MHz, 298 K, C_6D_6): δ=139.2 (C14), 114.5 (C15), 89.5 (C1), 68.8 (Cp), 68.4 (C2, C5), 67.5 (C3, C4), 34.2 (C13), 31.7 (C7), 30.0 (C6), 29.96, 29.89, 29.87 (C8, C9, C10), 29.5 (C11), 29.3 ppm (C12).

$Fc\text{-}CH_2\text{-}CH{=}CH\text{-}CH_2\text{-}Fc$ (4a): A solution of **3a** (0.71 g, 3.14 mmol) in toluene (20 mL) was added at once to a solution of $[Cl_2(PCy_3)_2Ru{=}CHPh]$ (0.29 g, 10 mol %) in toluene (10 mL) and stirred for 5 h at 60 °C under argon. The solvent was removed under reduced pressure, and the resulting red solid purified by column chromatography (pentane/toluene 9/1; R_f (**1**; **3a**)=0.6; R_f (**4a**)=0.2) (0.29 mg, 44 %). Single crystals of *trans*-**4a** suitable for X-ray analysis could be obtained from a concentrated $CHCl_3$ solution by slow evaporation of the solvent. M.p. 111 °C. ^{1}H NMR (599.8 MHz, 298 K, $CDCl_3$): δ=5.61 (m, 2 H; 7-H), 4.09 (s, 10 H; Cp-H), 4.05 (m, 8 H; 2,3,4,5-H), 3.03 ppm (m, 4 H; 6-H); ^{13}C NMR (150.8 MHz, 298 K, $CDCl_3$): δ=129.7 (C7), 87.9 (C1), 68.4 (Cp), 67.9 (C2, C5), 67.2 (C3, C4), 32.30 ppm (C6); elemental analysis calcd (%) for $C_{24}H_{24}Fe_2$ (M_r=424.14): C 67.96, H 5.70; found: C 67.58, H 5.61; MS (MALDI-TOF (DCTB)): *m/z* (%): 424.0 (100) [M^+]. X-ray crystal structure analysis of *trans*-**4a**: formula $C_{24}H_{24}Fe_2$, M_r=424.13, yellow crystal, 0.25×0.15×0.05 mm, a=11.173(1), b=9.783(1), c=8.411(1) Å, β=94.47(1)°, V=916.6(2) Å^3, ρ_{calcd}=1.537 g cm^{-3}, μ=15.87 cm^{-1}, empirical absorption correction (0.693≤T≤0.925), Z=2, monoclinic, space group $P2_1/c$ (no. 14), λ=0.71073 Å, T=198 K, ω and ϕ scans, 6780 reflections collected (±h, ±k, ±l), $\sin\theta/\lambda$=0.66 Å^{-1}, 2168 independent (R_{int}=0.038) and 1604 observed reflections [$I\geq 2\sigma(I)$], 118 refined parameters, R=0.033, wR_2=0.071, max. (min.) residual electron density 0.44 (−0.33) e Å^{-3}, hydrogen atoms calculated and refined as riding atoms.

$Fc\text{-}(CH_2)_3\text{-}CH{=}CH\text{-}(CH_2)_3\text{-}Fc$ (4b): Analogously to the procedure described for **4a**, compound **4b** was prepared using **3b** (0.76 g, 3.02 mmol) and $[Cl_2(PCy_3)_2Ru{=}CHPh]$ (0.25 g, 10 mol %). After column chromatography (pentane/toluene 4/1; R (**1**; **3b**)=0.75; R_f (**4b**)=0.45) compound **4b** was obtained as an orange solid (0.29 g, 35 %). Single crystals of *trans*-**4b** suitable for X-ray analysis could be obtained from a pentane/dichloromethane (4/1) solution at −30 °C. M.p. 53 °C. ^{1}H NMR (400.1 MHz, 300 K, $CDCl_3$): δ = 5.42 (m, 2H; 9-H), 4.01 (s, 10H; Cp-H), 4.06 (m, 4H; 2,5-H), 4.03 (m, 4H; 3,4-H), 2.32 (m, 4H; 6-H), 2.03 (m, 4H; 8-H), 1.57 ppm (m, 4H; 7-H); ^{13}C NMR (100.6 MHz, 300 K, $CDCl_3$): δ = 130.4 (C9), 89.3 (C1), 68.5 (Cp), 68.0 (C2, C5), 67.0 (C3, C4), 32.5 (C8), 31.0 (C7), 29.0 ppm (C6); elemental analysis calcd (%) for $C_{28}H_{32}Fe_2$ (M_r = 480.27): C 70.03, H 6.72; found: C 69.97, H 6.60; MS (MALDI-TOF (DCTB)): *m/z* (%): 480.2 (100) [M^+]. X-ray crystal structure analysis of *trans*-**4b**: formula $C_{28}H_{32}Fe_2$, M_r = 480.24, yellow crystal 0.25 × 0.15 × 0.05 mm, a = 25.938(1), b = 7.249(1), c = 12.340(1) Å, β = 90.78(1)°, V = 2320.0(4) Å^3, ρ_{calcd} = 1.375 g cm^{-3}, μ = 12.62 cm^{-1}, empirical absorption correction (0.743 ≤ T ≤ 0.940), Z = 4, monoclinic, space group $C2/c$ (no. 15), λ = 0.71073 Å, T = 198 K, ω and ϕ scans, 7374 reflections collected (±h, ±k, ±l), sinθ/λ = 0.66 Å^{-1}, 2774 independent (R_{int} = 0.054) and 1921 observed reflections [$I \geq 2\sigma(I)$], 140 refined parameters, R = 0.049, wR_2 = 0.123, max. (min.) residual electron density 0.73 (−0.44) e Å^{-3}, hydrogen atoms calculated and refined as riding atoms.

Fc-(CH$_2$)$_6$-CH=CH-(CH$_2$)$_6$-Fc (4c): Analogously to the procedure described for **4a**, compound **4c** was prepared using **3c** (0.73 g, 2.4 mmol) and [$Cl_2(PCy_3)_2Ru$=CHPh] (0.20 g, 10 mol %). After column chromatography (pentane/toluene 9/1; R (**1**; **3c**) = 0.6; R_f (**4c**) = 0.2) compound **4c** was obtained as a yellow solid (0.26 g, 38 %). Single crystals of *trans*-**4c** suitable for X-ray analysis could be obtained from a pentane solution at −30 °C. M.p. 50 °C. ^{1}H NMR (599.8 MHz, 298 K, $CDCl_3$): δ = 5.37 (m, 2H; 12-H); 4.07 (s, 10H; Cp-H), 4.03 (m, 4H; 2,5-H), 4.01 (m, 4H; 3,4-H), 2.29 (m, 4H; 6-H), 1.95 (m, 4H; 11-H), 1.47 (m, 4H; 7-H), 1.32 (m, 4H; 10-H), 1.29 ppm (m, 8H; 8,9-H); ^{13}C NMR (150.8 MHz, 298 K, $CDCl_3$): δ = 130.4 (C12), 89.5 (C1), 68.4 (Cp), 68.0 (C2, C5), 66.9 (C3, C4), 32.6 (C11), 31.1 (C7), 29.60, 29.57, 29.50 (C6, C8, C10), 29.0 ppm (C9); elemental analysis calcd (%) for $C_{34}H_{44}Fe_2$ (M_r = 564.4): C 72.35, H 7.86; found: C 72.45, H 7.96; MS (MALDI-TOF (DCTB)): *m/z* (%): 564.2 (100) [M^+]. X-ray crystal structure analysis of *trans*-**4c**: formula $C_{34}H_{44}Fe_2$, M_r = 564.39, yellow crystal, 0.15 × 0.03 × 0.03 mm, a = 14.944(1), b = 7.646(1), c = 13.286(1) Å, β = 111.76(1)°, V = 1409.9(2) Å^3, ρ_{calcd} = 1.329 g cm^{-3}, μ = 10.49 cm^{-1}, empirical absorption correction (0.859 ≤ T ≤ 0.969), Z = 2, monoclinic, space group $P2_1/c$ (no. 14), λ = 0.71073 Å, T = 198 K, ω and ϕ scans, 8956 reflections collected (±h, ±k, ±l), sinθ/λ = 0.59 Å^{-1}, 2470 independent (R_{int} = 0.110) and 1651 observed reflections [$I \geq 2\sigma(I)$], 163 refined parameters, R = 0.066, wR_2 = 0.156, max. (min.) residual electron density 0.47 (−0.43) e Å^{-3}, due to small size the crystals only diffract weakly, hydrogen atoms calculated and refined as riding atoms.

Fc-(CH$_2$)$_8$-CH=CH-(CH$_2$)$_8$-Fc (4d): Analogously to the procedure described for **4a**, compound **4d** was prepared using **3d** (1.5 g, 4.63 mmol) and [$Cl_2(PCy_3)_2Ru$=CHPh] (0.38 g, 10 mol %). After column chromatography (pentane/toluene 4/1; R_f (**1**; **3d**) = 0.7; R_f (**4d**) = 0.5) compound **4d** was obtained as yellow solid (0.37 g, 26 %). Single crystals of *trans*-**4d** suitable for X-ray analysis could be obtained from a pentane/CH_2Cl_2 solution (9/1) at −30 °C. M.p. 68.9 °C. ^{1}H NMR (599.8 MHz, 298 K, $CDCl_3$): δ = 5.37 (m, 2H; 14-H), 4.07 (s, 10H; Cp-H), 4.03 (m, 4H; 2,5-H), 4.02 (m, 4H; 3,5-H), 2.29 (m, 4H; 6-H), 1.95 (m, 4H; 13-H), 1.47 (m, 4H; 7-H), 1.31 (m, 4H; 12-H), 1.27 ppm (m, 16H; 8,9,10,11-H); ^{13}C NMR (150.8 MHz, 298 K, $CDCl_3$): δ = 130.3 (C14), 89.6 (C1), 68.4 (Cp), 68.0 (C2, C5), 67.0 (C3, C4), 32.6 (C13), 31.1 (C7), 29.65 (double intensity), 29.57, 29.50, 29.48, 29.16 ppm (C6, C8, C9, C10, C11, C12); elemental analysis calcd (%) for $C_{38}H_{52}Fe_2$ (M_r = 620.50): C 73.55, H 8.45; found: C 73.56, H 8.35; MS (MALDI-TOF (DCTB)): *m/z* (%): 620.1 (100) [M^+]. X-ray crystal structure analysis of *trans*-**4d**: formula $C_{38}H_{52}Fe_2$, M_r = 620.50, yellow crystal 0.20 × 0.15 × 0.03 mm, a = 15.892(1), b = 7.655(1), c = 13.186(1) Å, β = 92.07(1)°, V = 1603.1(3) Å^3, ρ_{calcd} = 1.285 g cm^{-3}, μ = 9.29 cm^{-1}, empirical absorption correction (0.836 ≤ T ≤ 0.973), Z = 2, monoclinic, space group $P2_1/c$ (no. 14), λ = 0.71073 Å, T = 198 K, ω and ϕ scans, 10451 reflections collected (±h, ±k, ±l), sinθ/λ = 0.66 Å^{-1}, 3778 independent (R_{int} = 0.119) and 2216 observed reflections [$I \geq 2\sigma(I)$], 181 refined parameters, R = 0.085, wR_2 = 0.185, max. (min.) residual electron density 0.46 (−0.65) e Å^{-3}, relatively poor quality of the data due to shape of crystals, hydrogen atoms calculated and refined as riding atoms.

Fc-(CH$_2$)$_{10}$-CH=CH-(CH$_2$)$_{10}$-Fc (*trans*-4e): *trans*-1,22-Dibromo-11-docosene (**7**, 0.30 g, 0.65 mmol) and lithioferrocene (**2**, 0.434 g, 2.2 mmol) were suspended in a mixture of toluene (10 mL) and tetrahydrofuran (5 mL) at −78 °C. The reaction mixture was allowed to warm to room temperature while stirring for 16 h. To quench the reaction it was poured into water and the aqueous phase was extracted three times with toluene. After drying over magnesium sulfate the crude product was purified by column chromatography (pentane/toluene 9/1; R_f (**1**) = 0.6; R_f (*trans*-**4e**) = 0.4). Compound *trans*-**4e** was obtained as a yellow solid (0.17 g, 39 %). Single crystals of *trans*-**4e** suitable for X-ray analysis could be obtained from a pentane/dichloromethane (2/1) solution at 5 °C. M.p. 83 °C. ^{1}H NMR (599.8 MHz, 298 K, C_6D_6): δ = 5.52 (m, 2H; 16-H), 4.03 (s, 10H; Cp-H), 4.00 (pt, 4H; 2,5-H), 3.97 (pt, 4H; 3,4-H), 2.29 (m, 4H; 6-H), 2.07 (m, 4H; 15-H), 1.53 (m, 4H; 7-H), 1.42 (m, 4H; 14-H), 1.33 (m, 4H; 13-H), 1.31 ppm (m, 20H; 8,9,10,11,12-H); ^{13}C NMR (150.8 MHz, 298 K, C_6D_6): δ = 130.8 (C16), 89.5 (C1), 68.8 (Cp), 68.4 (C2, C5), 67.5 (C3, C4), 33.1 (C15), 31.8 (C7), 30.11, 30.09, 30.08, 30.01 (double intensity), 29.99, 29.98 (C6, C8, C9, C10, C11, C12, C14), 29.6 ppm (C13); elemental analysis calcd (%) for $C_{42}H_{60}Fe_2$ (M_r = 676.64 g mol^{-1}): C 74.55, H 8.94; found: C 74.07, H 8.92; MS (MALDI-TOF (DCTB)): *m/z* (%) 676.6 (100) [M^+]. X-ray crystal structure analysis of *trans*-**4e**: formula $C_{42}H_{60}Fe_2$, M_r = 676.60, light yellow crystal, 0.15 × 0.10 × 0.03 mm, a = 18.072(1), b = 7.647(1), c = 13.241(1) Å, β = 103.06(1)°, V = 1782.5(3) Å^3, ρ_{calcd} = 1.261 g cm^{-3}, μ = 8.42 cm^{-1}, empirical absorption correction (0.884 ≤ T ≤ 0.975), Z = 2, monoclinic, space group $P2_1/c$ (no. 14), λ = 0.71073 Å, T = 198 K, ω and ϕ scans, 11674 reflections collected (±h, ±k, ±l), [(sinθ)/λ] = 0.66 Å^{-1}, 4215 independent (R_{int} = 0.095) and 2631 observed reflections [$I \geq 2\sigma(I)$], 199 refined parameters, R = 0.073, wR_2 = 0.135, max. (min.) residual electron density 0.35 (−0.62) e Å^{-3}, due to small size the crystals only diffract weakly, hydrogen atoms calculated and refined as riding atoms.

Fc-(CH$_2$)$_4$-Fc (5a): A solution of **4a** (0.15 g, 0.35 mmol) in tetrahydrofuran (10 mL) and Pd/C catalyst (15 mg) were stirred under 1 atm of H_2 for 3 h. After filtration over Celite and removal of the solvent, **5a** was isolated as a yellow solid. Single crystals of **5a** suitable for X-ray analysis could be obtained from a concentrated $CHCl_3$ solution by slow evaporation of the solvent. (0.14 g, 95 %). M.p. 117 °C. ^{1}H NMR (599.8 MHz, 298 K, $CDCl_3$): δ = 4.06 (s, 10H; Cp-H), 4.03 (m, 4H; 2,5-H), 4.01 (m, 4H; 3,4-H), 2.30 (m, 4H; 6-H), 1.51 ppm (m, 4H; 7-H); ^{13}C NMR (150.8 MHz, 298 K, $CDCl_3$): δ = 89.4 (C1), 68.5 (Cp), 68.0 (C2, C5), 67.0 (C3, C4), 31.1 (C7), 29.5 ppm (C6); elemental analysis calcd (%) for $C_{24}H_{26}Fe_2$ (M_r = 426.14): C 67.64, H 6.15; found: C 66.96, H 5.93. X-ray crystal structure analysis of **5a**: formula $C_{24}H_{26}Fe_2$, M_r = 426.15, yellow crystal 0.10 × 0.10 × 0.05 mm, a = 11.409(1), b = 9.730(1), c = 8.498(1) Å, β = 95.46(1)°, V = 939.1(2) Å^3, ρ_{calcd} = 1.507 g cm^{-3}, μ = 15.49 cm^{-1}, empirical absorption correction (0.861 ≤ T ≤ 0.927), Z = 2, monoclinic, space group $P2_1/c$ (no. 14), λ = 0.71073 Å, T = 198 K, ω and ϕ scans, 7507 reflections collected (±h, ±k, ±l), sinθ/λ = 0.66 Å^{-1}, 2215 independent (R_{int} = 0.044) and 1703 observed reflections [$I \geq 2\sigma(I)$], 118 refined parameters, R = 0.034, wR_2 = 0.075, max. (min.) residual electron density 0.41 (−0.31) e Å^{-3}, hydrogen atoms calculated and refined as riding atoms.

Fc-(CH$_2$)$_8$-Fc (5b): Analogously to the procedure described for **5a**, **5b** was prepared using **4b** (0.10 g, 0.21 mmol) and Pd/C catalyst (10 mg). After purification **5b** was obtained as a yellow solid (95 mg, 95 %). Single crystals of **5b** suitable for X-ray analysis could be obtained from a pentane/dichloromethane (10/1) solution at 5 °C. M.p. 96 °C. ^{1}H NMR (599.8 MHz, 298 K, C_6D_6): δ = 4.02 (s, 10H; Cp-H), 4.00 (pt, 4H; 2,5-H), 3.97 (pt, 4H; 3,4-H), 2.28 (m, 4H; 6-H), 1.52 (m, 4H; 7-H), 1.31 ppm (m, 8H; 8,9-H); ^{13}C NMR (150.8 MHz, 298 K, C_6D_6): δ = 89.6 (C1), 68.8 (Cp), 68.4 (C2, C5), 67.5 (C3, C4), 31.7 (C7), 30.01, 29.97, 29.93 ppm (C6, C8, C9); elemental analysis calcd (%) for $C_{28}H_{34}Fe_2$ (M_r = 482.28): C 69.73, H 7.11; found: C 69.36, H 7.27; MS (MALDI-TOF (DCTB)): *m/z* (%): 481.9 (100) [M^+]. X-ray crystal structure analysis of **5b**: formula $C_{28}H_{34}Fe_2$, M_r = 482.25, yellow crystal, 0.30 × 0.25 × 0.20 mm, a = 26.636(1), b = 7.608(1), c = 11.438(1) Å, β = 102.35(1)°, V = 2264.2(4) Å^3, ρ_{calcd} = 1.415 g cm^{-3}, μ = 12.94 cm^{-1}, empirical absorption correction (0.698 ≤ T ≤ 0.782), Z = 4, monoclinic, space group $C2/c$ (no. 15), λ = 0.71073 Å, T = 198 K, ω and ϕ scans, 7279 reflections collected (±h, ±k, ±l), sinθ/λ = 0.66 Å^{-1}, 2688 independent (R_{int} = 0.046) and 2285 observed reflections

$[I \geq 2\sigma(I)]$, 136 refined parameters, $R=0.033$, $wR_2=0.097$, max. (min.) residual electron density 0.36 (−0.46) e Å^{-3}, hydrogen atoms calculated and refined as riding atoms.

Fc-(CH$_2$)$_{14}$-Fc (5c): Analogously to the procedure described for **5a**, **5c** was prepared using **4c** (90 mg, 0.16 mmol) and Pd/C catalyst (10 mg). After purification **5c** was obtained as a yellow solid (90 mg, 99 %). Single crystals of **5c** suitable for X-ray analysis could be obtained from a pentane solution at 5 °C. M.p. 94 °C. ^{1}H NMR (599.8 MHz, 298 K, CDCl$_3$): $\delta=4.07$ (s, 10H; Cp-H), 4.03 (m, 4H; 2,5-H), 4.01 (m, 4H; 3,4-H), 2.29 (m, 4H; 6-H), 1.47 (m, 4H; 7-H), 1.27 (m, 4H; 8-H), 1.25 ppm (m, 16H; 9,10,11,12-H); ^{13}C NMR (150.8 MHz, 298 K, CDCl$_3$): $\delta=89.6$ (C1), 68,4 (Cp), 68.1 (C2, C5), 66.9 (C3, C4), 31.1 (C7), 29.67 (triple intensity), 29.64, 29.57, 29.55 ppm (C6, C8, C9, C10, C11, C12); elemental analysis calcd (%) for $C_{34}H_{46}Fe_2$ ($M_r=566.43$): C 72.10, H 8.19; found: C 72.55, H 8.25; MS (MALDI-TOF (DCTB)): *m/z* (%): 566.1 (100) [M^+]. X-ray crystal structure analysis of **5c**: formula $C_{34}H_{46}Fe_2$, $M=566.41$, yellow crystal $0.35\times0.15\times0.03$ mm, $a=16.785(1)$, $b=7.587(1)$, $c=11.225(1)$ Å, $\beta=95.28(1)°$, $V=1423.4(2)$ Å^3, $\rho_{calcd}=1.322$ g cm^{-3}, $\mu=10.40$ cm^{-1}, empirical absorption correction ($0.712\leq T\leq0.970$), $Z=2$, monoclinic, space group $P2_1/c$ (no. 14), $\lambda=0.71073$ Å, $T=198$ K, ω and ϕ scans, 8593 reflections collected ($\pm h$, $\pm k$, $\pm l$), $[(\sin\theta)/\lambda]=0.62$ Å^{-1}, 2877 independent ($R_{int}=0.082$) and 2046 observed reflections $[I\geq2\sigma(I)]$, 163 refined parameters, $R=0.053$, $wR_2=0.119$, max. (min.) residual electron density 0.51 (−0.33) e Å^{-3}, hydrogen atoms calculated and refined as riding atoms.

Fc-(CH$_2$)$_{18}$-Fc (5d): Analogously to the procedure described for **5a**, compound **5d** was prepared using **4d** (70 mg, 0.11 mmol) and Pd/C catalyst (10 mg). After purification compound **5d** was obtained as a yellow solid (70 mg, 99 %). Single crystals of **5d** suitable for X-ray analysis could be obtained from a heptane/CH$_2$Cl$_2$ solution (5/1) at −30 °C. M.p. 73 °C. ^{1}H NMR (599.8 MHz, 298 K, C$_6$D$_6$): $\delta=4.03$ (s, 10H; Cp-H), 4.00 (pt, 4H; 2,5-H), 3.97 (pt, 4H; 3,4-H), 2.29 (m, 4H; 6-H), 1.53 (m, 4H; 7-H), 1.34 ppm (m, 28H; 8,9,10,11,12,13,14-H); ^{13}C NMR (150.8 MHz, 298 K, C$_6$D$_6$): $\delta=89.5$ (C1), 68.8 (Cp), 68.4 (C2, C5), 67.5 (C3, C4), 31.7 (C7), 30.17 (double intensity), 30.16, 30.14, 30.11, 30.01, 30.00 ppm (double intensity, C6, C8–C14); elemental analysis calcd (%) for $C_{38}H_{54}Fe_2$ ($M_r=622.51$): C 73.32, H 8.74; found: C 73.05, H 9.00; MS (MALDI-TOF (DCTB)): *m/z* (%): 622.3 (100) [M^+]. X-ray crystal structure analysis of **5d**: formula $C_{38}H_{54}Fe_2$, $M_r=622.51$, yellow crystal, $0.30\times0.25\times0.03$ mm, $a=19.119(1)$, $b=7.591(1)$, $c=11.267(1)$ Å, $\beta=99.14(1)°$, $V=1614.4(3)$ Å^3, $\rho_{calcd}=1.281$ g cm^{-3}, $\mu=9.23$ cm^{-1}, empirical absorption correction ($0.769\leq T\leq0.973$), $Z=2$, monoclinic, space group $P2_1/c$ (no. 14), $\lambda=0.71073$ Å, $T=198$ K, ω and ϕ scans, 8744 reflections collected ($\pm h$, $\pm k$, $\pm l$), $\sin\theta/\lambda=0.67$ Å^{-1}, 3939 independent ($R_{int}=0.057$) and 2832 observed reflections $[I\geq2\sigma(I)]$, 181 refined parameters, $R=0.072$, $wR_2=0.156$, max. (min.) residual electron density 0.75 (−0.39) e Å^{-3}, hydrogen atoms calculated and refined as riding atoms.

Fc-(CH$_2$)$_{22}$-Fc (5e): Analogously to the procedure described for **5a**, **5e** was prepared using **4e** (90 mg, 0.13 mmol) and Pd/C catalyst (10 mg). After purification **5e** was obtained as a yellow solid (85 mg, 94 %). Single crystals of **5e** suitable for X-ray analysis could be obtained from a heptane/CH$_2$Cl$_2$ solution (2/1) at 5 °C. M.p. 104 °C. ^{1}H NMR (599.8 MHz, 298 K, C$_6$D$_6$): $\delta=4.03$ (s, 10H; Cp-H), 4.00 (pt, 4H; 2,5-H), 3.97 (pt, 4H; 3,4-H), 2.28 (m, 4H; 6-H), 1.53 (m, 4H; 7-H), 1.34 ppm (m, 36H; 8,9,10,11,12,13,14,15,16-H); ^{13}C NMR (150.8 MHz, 298 K, C$_6$D$_6$): $\delta=89.5$ (C1), 68.8 (Cp), 68.4 (C2, C5), 67.5 (C3, C4), 31.8 (C7), 30.17 (triple intensity), 30.16, 30.15, 30.11, 30.02, 30.01 ppm (double intensity, C6, C8–C16); elemental analysis calcd (%) for $C_{42}H_{62}Fe_2$ ($M_r=678.65$): C 74.33, H 9.21; found: C 73.64, H 9.30; MS (MALDI-TOF (DCTB)): *m/z* (%): 678.4 (100) [M^+]. X-ray crystal structure analysis of **5e**: formula $C_{42}H_{62}Fe_2$, $M_r=678.62$, yellow crystal $0.25\times0.20\times0.03$ mm, $a=21.407(1)$, $b=7.551(1)$, $c=11.248(1)$ Å, $\beta=99.91(1)°$, $V=1791.0(3)$ Å^3, $\rho_{calcd}=1.258$ g cm^{-3}, $\mu=8.38$ cm^{-1}, empirical absorption correction ($0.818\leq T\leq0.975$), $Z=2$, monoclinic, space group $P2_1/c$ (no. 14), $\lambda=0.71073$ Å, $T=198$ K, ω and ϕ scans, 16644 reflections collected ($\pm h$, $\pm k$, $\pm l$), $\sin\theta/\lambda=0.66$ Å^{-1}, 4257 independent ($R_{int}=0.058$) and 3322 observed reflections $[I\geq2\sigma(I)]$, 199 refined parameters, $R=0.058$, $wR_2=0.151$, max. (min.) residual electron density 0.76 (−0.56) e Å^{-3}, hydrogen atoms calculated and refined as riding atoms.

Fc-(CH$_2$)$_{12}$-Fc (5f): Lithioferrocene (**2**) was prepared in situ from ferrocene (**1**, 9.35 g, 50 mmol) and *tert*-butyllithium (1.5 M in pentane, 34 mL, 50 mmol) in tetrahydrofuran (70 mL) under argon. The resulting suspension was cooled to −78 °C and a solution of 1,12-dibromododecane (5.00 g, 15.3 mmol) in tetrahydrofuran (30 mL) was added dropwise. The suspension was stirred for 16 h while slowly warming to room temperature. The residue was dissolved in pentane, the solvent volume reduced, and the remaining ferrocene was allowed to crystallize out of the mixture. Compound **5f** remained in solution. Afterwards the crude product was purified by column chromatography on silica gel (pentane/toluene 17/3). The second fraction was collected. (R_f (**1**)$=0.7$; R_f (**5f**)$=0.5$). After evaporation of the solvent **5f** was obtained as an orange solid (2.20 g, 27 %). Single crystals of **5f** suitable for X-ray analysis could be obtained from a heptane/CH$_2$Cl$_2$ solution (5/1) at 5 °C. M.p. 92 °C. ^{1}H NMR (599.8 MHz, 298 K, C$_6$D$_6$): $\delta=4.03$ (s, 10H; Cp-H), 4.00 (pt, 4H; 2,5-H), 3.97 (pt, 4H; 2,5-H), 2.23 (m, 4H; 6-H), 1.53 (m, 4H; 7-H), 1.33 ppm (m, 16H; 8,9,10,11-H); ^{13}C NMR (150.8 MHz, 298 K, C$_6$D$_6$): $\delta=89.5$ (C1), 68.8 (Cp), 68.4 (C2, C5), 67.5 (C3, C4), 31.7 (C7), 30.12, 30.09, 30.00 (double intensity), 29.99 ppm (C6, C8–C11); elemental analysis calcd (%) for $C_{32}H_{42}Fe_2$ ($M_r=538.39$): C 71.39, H 7.86; found: C 71.48, H 7.84; MS (MALDI-TOF (DCTB)): *m/z* (%) 538.2 (100) [M^+]. X-ray crystal structure analysis for **5f**: formula $C_{32}H_{42}Fe_2$, $M_r=538.36$, yellow crystal $0.25\times0.25\times0.05$ mm, $a=16.265(1)$, $b=7.657(1)$, $c=11.276(1)$ Å, $\beta=104.07(1)°$, $V=1362.2(2)$ Å^3, $\rho_{calcd}=1.313$ g cm^{-3}, $\mu=10.83$ cm^{-1}, empirical absorption correction ($0.774\leq T\leq0.948$), $Z=2$, monoclinic, space group $P2_1/c$ (no. 14), $\lambda=0.71073$ Å, $T=293$ K, ω and ϕ scans, 10515 reflections collected ($\pm h$, $\pm k$, $\pm l$), $\sin\theta/\lambda=0.67$ Å^{-1}, 3342 independent ($R_{int}=0.050$) and 2270 observed reflections $[I\geq2\sigma(I)]$, 154 refined parameters, $R=0.037$, $wR_2=0.095$, max. (min.) residual electron density 0.20 (−0.34) e Å^{-3}, hydrogen atoms calculated and refined as riding atoms.

Br-(CH$_2$)$_{10}$-CH=CH-(CH$_2$)$_{10}$-Br (7): A solution of 1-bromo-11-dodecene (**6**, 1.72 g, 6.97 mmol) in toluene (40 mL) was added at once to a solution of [Cl$_2$(PCy$_3$)$_2$Ru=CHPh] (57 mg, 1 mol %) in toluene (5 mL) and stirred for 12 h at room temperature. The solvent was removed under reduced pressure and the resulting solid was purified by column chromatography. (pentane, R_f (**7**)$=0.3$) (1.27 g, 78 %, *cis*/*trans* mixture). Recrystallization from a heptane solution of **7** at 5 °C gave the pure *trans* product (0.53 g, 33 %). M.p. 49 °C. ^{1}H NMR (599.8 MHz, 298 K, C$_6$D$_6$): $\delta=5.53$ (m, 2H; 11-H), 2.97 (t, $^3J_{H,H}=7.0$ Hz, 4H; 1-H), 2.08 (m, 4H; 10-H), 1.51 (m, 4H; 2-H), 1.41 (m, 4H; 9-H), 1.32 (m, 4H; 8-H), 1.26 (m, 4H; 7-H), 1.21 (m, 4H; 6-H), 1.15 (m, 8H; 3,5-H), 1.07 ppm (m, 4H; 4-H); ^{13}C NMR (150.8 MHz, 298 K, C$_6$D$_6$): $\delta=130.8$ (C11), 33.7 (C1), 33.1 (C10), 33.0 (C2), 30.1 (C9), 29.9 (C6, C7), 29.7 (C5), 29.6 (C8), 29.0 (C4), 28.3 ppm (C3); elemental analysis calcd (%) for $C_{22}H_{42}Br_2$ ($M_r=466.38$): C 56.66, H 9.08; found: C 56.22, H 8.95.

Acknowledgement

Financial support from the Deutsche Forschungsgemeinschaft and the Fonds der Chemischen Industrie is gratefully acknowledged.

---

[1] a) D. M. Cyr, B. Venkataraman, G. W. Flynn, *Chem. Mater.* **1996**, *8*, 1600–1615; b) S. De Feyter, A. Gesquiére, M. M. Abdel-Mottaleb, P. C. M. Grim, F. C. De Schryver, C. Meiners, M. Sieffert, S. Valiyaveettil, K. Müllen, *Acc. Chem. Res.* **2000**, *33*, 520–531.

[2] a) G. C. McGonigal, R. H. Bernhadt, D. J. Thomson, *Appl. Phys. Lett.* **1990**, *57*, 28–30; b) J. P. Rabe, S. Buchholz, *Science* **1991**, *253*, 424–427.

[3] a) X. Lu, K. W. Hipps, *J. Phys. Chem. B* **1997**, *101*, 5391–5396; b) L. Scudiero, D. E. Barlow, K. W. Hipps, *J. Phys. Chem. B* **2000**, *104*, 11899–11905; c) K. T. Wong, J. M. Lehn, S. M. Peng, G. H. Lee, *Chem. Commun.* **2000**, *22*, 2259–2260; d) X. Qiu, C. Wang, S. Yin,

Q. Zeng, B. Xu, C. Bai, *J. Phys. Chem. B* **2000**, *104*, 3570–3574; e) L. Scudiero, D. E. Barlow, U. Mazur, K. W. Hipps, *J. Am. Chem. Soc.* **2001**, *123*, 4073–4080; f) M. M. S. Abdel-Mottaleb, N. Schuurmans, S. De Feyter, J. Van Esch, B. L. Feringa, F. C. De Schryver, *Chem. Commun.* **2002**, 1894–1895; g) U. Ziener, J. M. Lehn, A. Mourran, M. Moller, *Chem. Eur. J.* **2002**, *8*, 951–957; h) S. Yin, C. Wang, B. Xu, C. Bai, *J. Phys. Chem. B* **2002**, *106*, 9044 –9047; i) S. Hoeppener, J. Wonnemann, L. Chi, G. Erker, H. Fuchs, *ChemPhysChem* **2003**, *4*, 490–494.

[4] a) S. T. Nguyen, L. K. Johnson, R. H. Grubbs, *J. Am. Chem. Soc.* **1992**, *114*, 3974–3975; b) S. T. Nguyen, R. H. Grubbs, J. W. Ziller, *J. Am. Chem. Soc.* **1993**, *115*, 9858–9859; c) P. Schwab, M. B. France, J. W. Ziller, R. H. Grubbs, *Angew. Chem.* **1995**, *107*, 2179–2181; *Angew. Chem. Int. Ed. Engl.* **1995**, *34*, 2039–2041; d) P. Schwab, R. H. Grubbs, J. W. Ziller, *J. Am. Chem. Soc.* **1996**, *118*, 100–110; e) M. Schuster, S. Blechert, *Angew. Chem.* **1997**, *109*, 2124–2144; *Angew. Chem. Int. Ed. Engl.* **1997**, *36*, 2037–2056; f) R. H. Grubbs, S. Chang, *Tetrahedron* **1998**, *54*, 4413–4450; g) A. Fürstner, *Angew. Chem.* **2000**, *112*, 3140–3172; *Angew. Chem. Int. Ed.* **2000**, *39*, 3013–3043; h) *Handbook of Metathesis, Vols. 1–3* (Ed.: R. H. Grubbs), Wiley-VCH, Weinheim, **2003**.

[5] a) C. Alvarez Toledano, A. Parlier, H. Rudler, J.-C. Daran, Y. Jeannin, *J. Chem. Soc. Chem. Commun.* **1984**, 576–578; b) C. Alvarez, A. Pacreau, A. Parlier, H. Rudler, J.-C. Daran, *Organometallics* **1987**, *6*, 1057–1064; c) B. Mohr, M. Weck, J.-P. Sauvage, R. H. Grubbs, *Angew. Chem.* **1997**, *109*, 1365–1367; *Angew. Chem. Int. Ed. Engl.* **1997**, *36*, 1308–1310; d) M. Weck, B. Mohr, J.-P. Sauvage, R. H. Grubbs, *J. Org. Chem.* **1999**, *64*, 5463–5471; e) H. E. Blackwell, D. J. O'Leary, A. K. Chatterjee, R. A. Washenfelder, D. A. Bussmann, R. H. Grubbs, *J. Am. Chem. Soc.* **2000**, *122*, 58–71; f) J. Ruwwe, J. M. Martin-Alvarez, C. R. Horn, E. B. Bauer, S. Szafert, T. Lis, F. Hampel, P. C. Cagle, J. A. Gladysz, *Chem. Eur. J.* **2001**, *7*, 3931–3950; g) C. R. Horn, J. M. Martin- Alvarez, J. A. Gladysz, *Organometallics* **2002**, *21*, 5386–5393; h) T. Yasuda, J. Abe, H. Yoshida, T. Iyoda, T. Kawai, *Adv. Synth. Catal.* **2002**, *344*, 705–711; i) M. Ogasawara, T. Nagano, T. Hayashi, *J. Am. Chem. Soc.* **2002**, *124*, 9068–9069; j) M. Ogasawara, T. Nagano, T. Hayashi, *Organometallics* **2003**, *22*, 1174–1176; k) T. Shima, F. Hampel, J. A. Gladysz, *Angew. Chem.* **2004**, *116*, 5653–5656; *Angew. Chem. Int. Ed.* **2004**, *43*, 5537–5540.

[6] a) D. Hüerländer, N. Kleigrewe, G. Kehr, G. Erker, R. Fröhlich, *Eur. J. Inorg. Chem.* **2002**, 2633–2642; b) J. Cano Sierra, D. Hüerländer, M. Hill, G. Kehr, G. Erker, R. Fröhlich, *Chem. Eur. J.* **2003**, *9*, 3618–3622; c) G. Erker, G. Kehr, R. Fröhlich, *J. Organomet. Chem.* **2004**, *689*, 1402–1412.

[7] M. Herberhold, A. Ayazi, W. Milius, B. Wrackmeyer, *J. Organomet. Chem.* **2002**, *656*, 71–80.

[8] M. Roux, R. Paugam, G. Rousseau, *J. Org. Chem.* **2001**, *66*, 4304–4310.

[9] The calculations were performed with the TURBOMOLE 5.6 suite of programs (Universität Karlsruhe, **2003**). The structures were fully optimized at the density functional (DFT) level employing the BLYP functional (A. D. Becke, *Phys. Rev. A* **1988**, *38*, 3098–3100. C. Lee, W. Yang, R. G. Parr, *Phys. Rev. B* **1988**, *37*, 785–789). A Gaussian AO basis of valence-triple-zeta quality including polarization functions (TZVP) (A. Schäfer, C. Huber, R. Ahlrichs, *J. Chem. Phys.* **1994**, *100*, 5829–5835) was used for all atoms. The RI approximation was used for the two-electron integrals (K. Eichkorn, O. Treutler, H. Öhm, M. Häser, R. Ahlrichs, *Chem. Phys. Lett.* **1995**, *240*, 283–290).

[10] S. Grimme, *J. Comput. Chem.* **2004**, *25*, 1463–1473. Parameters for iron in the calculation of the dispersion energy and the damping function: $C_6 = 10.0\,\mathrm{J\,nm^6\,mol^{-1}}$, $R_0 = 174$ pm.

[11] *The CH/π-Interaction; Evidence, Nature, and Consequences: M. Nishio, M. Hirota, Y. Umezawa in Methods in Stereochemical Analysis* (Ed.: A. P. Marchand), Wiley-VCH, New York, **1998**.

[12] a) P. C. M. Grim, S. De Feyter, A. Gesquiére, P. Vanoppen, M. Rucker, S. Valiyaveettil, G. Moessner, K. Müllen, F. C. De Schryver, *Angew. Chem.* **1997**, *109*, 2713–2715; *Angew. Chem. Int. Ed. Engl.* **1997**, *36*, 2601–2603; b) Y. Okawa, M. Aono, *Nature* **2001**, *409*, 683–684; c) Y. Okawa, M. Aono, *J. Chem. Phys.* **2001**, *115*, 2317–2322; d) S. De Feyter, J. Hofkens, M. van der Auweraer, R. J. M. Nolte, K. Müllen, F. C. De Schryver, *Chem. Commun.* **2001**, 585–592; e) A. Miura, S. De Feyter, M. M. S. Abdel-Mottaleb, A. Gesquiére, P. C. M. Grim, G. Moessner, M. Sieffert, M. Klapper, K. Müllen, F. C. De Schryver, *Langmuir* **2003**, *19*, 6474–6482.

[13] S. Berger, S. Braun, *200 and More NMR Experiments: A Practical Course*, 3rd ed., Wiley-VCH, Weinheim, **2004**, and references therein.

[14] I. J. Bruno, J. C. Cole, P. R. Edgington, M. K. Kessler, C. F. Macrae, P. McCabe, J. Pearson, R. Taylor, *Acta Crystallogr. Sect. B* **2002**, *58*, 389–397.

Received: May 18, 2005